tions will soon be performed.

In the work presented above we delineated the importance of collisional quenching in the measurements of x-ray spectra from projectiles moving in various targets. These spectra provide unique opportunities to study the long-range interaction of neutral atoms with highly ionized atoms. This work also demonstrates that previous measurements[2] of the spectral intensities following a single inner-shell collision have been obscured by the use of high gas densities. While the work described here is only for the heliumlike atoms the effects of collisional quenching will not be unique to these systems. Indeed we have observed similar effects for the lithiumlike transitions. Moreover, the present measurements give only the total quenching cross sections. Detailed information on how the $^3P_1$ state is quenched (i.e., what final states are preferred) cannot be determined from these measurements. Detailed information on the quenching of other long-lived states such as 2^3P_0, 2^3P_2, and 2^3S_1 might also be useful. Theoretical calculations for the rates of possible transitions out of these metastable states during energetic ion-atom collisions are needed.

The charge-state dependence presented in Fig. 2 indicates that additional experiments, in which the metastable beam components have been separated or removed by natural decay, will be necessary to determine the importance of Coulomb excitation in populating these states.

*Work performed under the auspices of the U. S. Energy Research and Development Administration.

†Summer visitor on leave from East Carolina University, Greenville, N. C. 27834.

[1]H. S. W. Massey and E. H. S. Burhop, *Electronic and Ionic Impact Phenomena* (Clarendon Press, Oxford, England, 1952), pp. 417–440; J. B. Hasted, *Physics of Atomic Collisions* (Butterworths, London, 1964), pp. 449–453.

[2]J. R. MacDonald, P. Richard, C. L. Cocke, M. Brown, and I. A. Sellin, Phys. Rev. Lett. 31, 684 (1973); F. Hopkins, R. L. Kauffman, C. W. Woods, and P. Richard, Phys. Rev. A 9, 2419 (1974).

[3]J. R. Mowat, I. A. Sellin, R. S. Peterson, M. O. Brown, and J. R. MacDonald, Phys. Rev. Lett. 30, 1289 (1973).

[4]Forrest Hopkins, private communication.

[5]R. Marrus, Nucl. Instrum. Methods 110, 333 (1973).

Spectral Resolution of Near-Resonant Rayleigh Scattering and Collision-Induced Resonance Fluorescence*

J. L. Carlsten and A. Szöke†

Joint Institute for Laboratory Astrophysics, University of Colorado and National Bureau of Standards, Boulder, Colorado 80309

(Received 1 December 1975)

Light scattered from strontium vapor near its 460.73-nm ($^1P_1°$–$^1S_0$) resonance transition was resolved into its three spectral components: Rayleigh scattering, collision-induced fluorescence, and three-photon scattering. The saturation behavior of the central (Rayleigh) component and the intensity and ac Stark shift of the three-photon component were studied as a function of detuning and laser intensity. Good agreement is obtained with theoretical predictions.

Spectral analysis of near-resonance scattering of narrow-band light by atomic vapors has held the interest of physicists for many years.[1,2] At low light intensities when collisions are present, the spectrum consists of two components,[3,4] while at high intensities three components are resolvable.[5] The frequency of the central component is centered on the incident frequency ω_L, the second component is centered on $\omega_0+\delta=\omega_L+(\Delta+\delta)$ (where ω_0 is the resonance frequency of the transition, $\Delta=\omega_0-\omega_L$ is the detuning and δ is the shift due to the ac Stark effect), and the third component, that appears at higher intensities, is symmetrically located on the other side of the incident frequency at $\omega_L-(\Delta+\delta)$. It is convenient to call these components Rayleigh scattering, fluorescence, and three-photon scattering, respectively. This Letter reports the first spectrally resolved observation of the collisionally induced fluorescence component, as well as a study of the saturation behavior of the Rayleigh component at high laser intensities. In the experiment, a dye laser was tuned near the 460.73-nm ($^1P°$–^1S) resonance line in strontium vapor and the light scat-

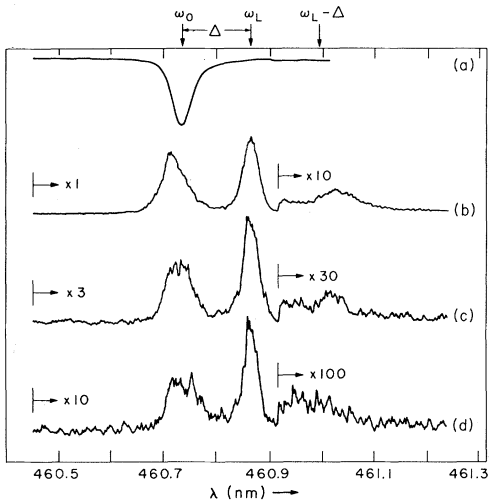

FIG. 1. (a) Absorption profile of the Sr. atomic resonance at 460.73 nm. The other traces show spectral scans of the side emission with the laser attenuated by (b) 0.0, (c) 0.45, and (d) 1.0 neutral density filters. The factors show the increase in sensitivity.

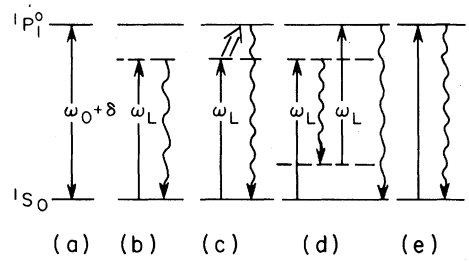

FIG. 2. (a) Simplified energy levels for Sr in the laser field; schematic mechanisms of (b) Rayleigh scattering at ω_L, (c) collision-induced fluorescence at $\omega_0 + \delta$, (d) "three-photon" scattering at $\omega_L - (\Delta + \delta)$ and consequent fluorescence at $\omega_0 + \delta$, and (e) nonadiabatic excitation leading to fluorescence at $\omega_0 + \delta$. Strong fields, represented by full lines, have to be treated nonperturbatively; scattered photons, symbolized by wavy lines, can be treated to first order.

tered to the side was analyzed by a monochromator. We observed the redistribution process[4] that is of importance to problems of radiative energy transport.[6] Several recent experiments have some relation to our work.[7-15]

The theory of resonance scattering in the absence of saturation, but including collisions, is well understood in the impact limit.[3,4,16] There are also several fundamental theories of scattering at arbitrary (high) incident light intensities when the damping is purely radiative; a general consensus exists among them.[17-20] However, when both saturation and collision effects are important, the theory is in its infancy.[21]

We have used a tunable dye laser, pumped by an N_2 laser,[22] to study the emission components discussed above. The dye laser had a pulse width of 5 nsec, a full-angle beam divergence of 2 mrad, a spectral width of 0.03 nm, and an energy of 0.2 mJ at the oven entrance; it was run at a repetition rate of 2 pulses/sec. The beam was focused into a strontium oven which contained typically 37 Torr of argon buffer gas. The absorption profile, Fig. 1(a), taken with a tungsten filament lamp had an equivalent width of 0.03 nm and the number density of the strontium atoms was $3\times10^{13}/\mathrm{cm}^3$, as determined by a curve-of-growth method.[23] The diameter of the excitation region was 2.2 mm, as measured by scanning the focusing lens, giving a peak power of 2.1 $\mathrm{MW/cm}^2$. The emission region was imaged onto the slit of a 300-mm monochromator of 0.03 nm resolution with an $f/10$ optical system. The output of the photomultiplier, placed at the exit of the monochromator, was fed into a gated (10 μsec) analog integrate-and-hold circuit (to eliminate dark current) and recorded on a chart recorder with a 1.5-sec time constant. The wavelength reproducibility from scan to scan was 0.01 nm.

A composite picture of spectral scans, taken under the above conditions, is shown in Fig. 1. The laser was set 0.13 nm from the resonance line on the long-wavelength side. The absorption profile, Fig. 1(a), shows the spectral location of the unperturbed atomic resonance, and Figs. 1(b)–1(d) show the emission for full laser intensity, and for the laser attenuated by 0.45 and 1.0 neutral density filters, respectively. The three components are clearly resolved; a discussion of some of their properties, obtained from many similar scans, constitutes the rest of the paper.

The central (Rayleigh) component appears at 460.86 nm in Fig. 1 and its mechanism is shown schematically in Fig. 2(b). Its center frequency coincides with the incident frequency, ω_L, as predicted by theory (seen also in Refs. 5, 11, and 12). At low intensities the Rayleigh scattering is coherent,[3,4] so that for stationary atoms the emission is as narrow as the incident laser. At higher intensities, even in the absence of collisions, there is also a noncoherent part to the Rayleigh scattering which has a spectral width equal to the natural width.[18,19] In the absence of collisions, the integrated intensity of this central component, I_R (the sum of the coherent and incoherent parts, in photons per cubic centime-

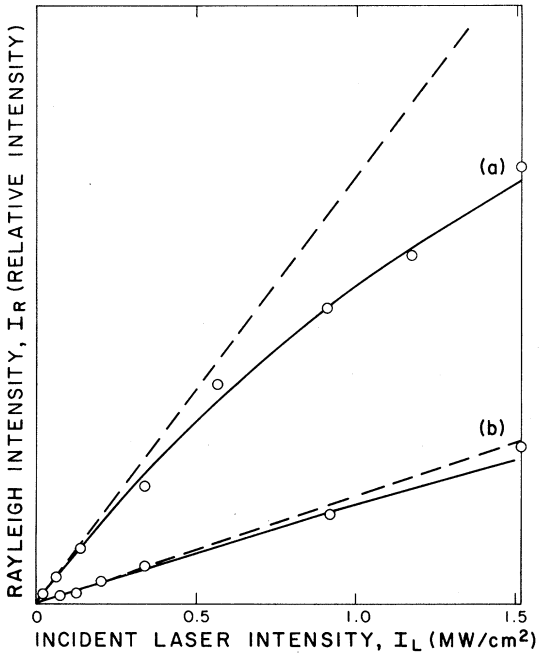

FIG. 3. Dependence of the intensity of the Rayleigh component I_R on the incident laser intensity I_L for two values of detuning: (a) 0.13 nm, (b) 0.26 nm. The solid curves are theory based on Eq. (1). The dashed curves are extrapolations from the linear dependence at low intensities.

ter per second), is[18,21]

$$I_R = N(\gamma_N/2)\Omega^2/(\Delta^2+\gamma_N^2+\Omega^2), \quad (1)$$

where N is the density of the strontium atoms, γ_N is the natural linewidth, $\Omega = \mu E/\hbar$ is the (instantaneous) Rabi frequency associated with the incident laser field $\vec{E}(t) = \hat{\epsilon}_L E(t)\cos\omega t$, $\hat{\epsilon}_L$ is the laser's polarization vector, and $\mu = e\langle 2|\hat{\epsilon}_L \cdot \vec{r}|1\rangle$. Note that $\Omega^2 \propto I_L$, where I_L is the incident laser intensity. The low-intensity limit of this expression coincides with that of Huber[3] and Omont, Smith, and Cooper[4] with γ_N in the denominator of Eq. (1) replaced by $\gamma_N + \gamma_C$, where γ_C is the rate of collisions.

In the high-intensity limit Eq. (1) predicts the saturation of the Rayleigh scattering. This is well borne out by our experimental results, shown in Fig. 3. The intensity I_R of the Rayleigh component is plotted as a function of the incident laser intensity I_L. Figure 3(a) was taken with the laser tuned to 0.13 nm to the long-wavelength side away from resonance, and Fig. 3(b), with a detuning of 0.26 nm. The solid curve in Fig. 3(a) was calculated using Eq. (1) with the incident laser intensity and the overall gain of the detection system as free parameters. The best fit was for an average laser intensity of 1.5 MW/cm²[24] as compared with our measured value of 2.1 MW/cm². A simple change of Δ to 0.26 nm gave the solid curve of Fig. 3(b) that fits the relevant data equally well. At low intensities the data in Fig. 3 show the expected $1/\Delta^2$ dependence. This $1/\Delta^2$ dependence of the Rayleigh intensity and its independence on the sign of Δ was verified by us for detunings up to $\Delta = 1$ nm. Also, I_R was found to be proportional to strontium density as expected from Eq. (1). The effect of saturation is apparent at high intensities where the Rayleigh component falls below the linear curve. It is more pronounced closer to resonance, as predicted by Eq. (1). We have observed even more saturation when the laser was tightly focused, but spatial inhomogeneities of the laser beam caused I_R to increase by a factor of 2 over that predicted by Eq. (1).

The third component which appears at ~461.0 nm in Fig. 1 corresponds to the "three-photon" process depicted by Fig. 2(d).[24] The total intensity of this component in the collisionless case is given by[18]

$$I_3 = \frac{N(\gamma_N/8)\Omega^4}{(\Delta^2+\gamma_N^2+\Omega^2)(\Delta^2+\gamma_N^2+\Omega^2/2)} \quad (2)$$

As mentioned above, this third component is centered on $\omega_L - (\Delta+\delta)$, where δ is the ac Stark shift given by[18,19,21]

$$\delta = \Delta\{[1+(\Omega/\Delta)^2]^{1/2}-1\}, \quad (3)$$

and observed in Refs. 5 and 13–15. Since our laser field is nonuniform and pulsed, the shift shows up both as an average shift and as a broadening.

We have observed the third component at its predicted position for both positive and negative values of the detuning Δ and for various laser intensities. Using the laser intensity and overall gain of the detection system determined by the theoretical fit to the Rayleigh saturation data (Fig. 3), we obtained a prediction with no adjustable parameters for both the total intensity of the third component by Eq. (2) and the ac Stark shift by Eq. (3). Agreement was within our 20% experimental error. The measured shift at full laser intensity was 0.03 nm. It is interesting (but expected from Ref. 21) that the collisionless formulas of Eqs. (1)–(3) are applicable to our experimental situation, where the collision rate is an order of magnitude larger than the radiative decay rate, but the detuning is much larger than the homogeneous linewidth ($\Delta >> \gamma_N + \gamma_C$).

The fluorescence component at ~460.7 nm is prominent in Fig. 1 and is clearly resolved from the central (Rayleigh) component. At high laser intensities it is shifted and asymmetric as a result of the ac Stark effect. At low intensities and large detunings, it is centered on the unperturbed atomic transition.

There are three processes which can give rise to this fluorescence component. In strong fields, it can occur as a consequence of the three-photon process discussed above [Fig. 2(d)]. Since this process leads to an actual population of the $^1P_1^\circ$ level, a resonance photon will be spontaneously emitted some time later as a result of radiative damping, contributing an intensity comparable to I_3 to the fluorescence component. Secondly, if the incident light is not monochromatic but has spectral wings at the resonance frequency, nonadiabatic excitation[26] can occur as shown schematically in Fig. 2(e). The third way the fluorescence component can arise is by collisional transfer from the laser-excited virtual level [Fig. 2(c)].

Since the strontium oven had an optical depth of ~800 any spectral components at the resonant frequency were totally absorbed by the strontium vapor surrounding the excitation region. Therefore at low laser intensities when the ac Stark shift is less than the equivalent width[23] of the absorption line (~0.03 nm) nonadiabatic excitation could not have been occurring. In addition, fluorescence at $\omega_0 + \delta$ due to excitation by the three-photon process was negligible (< 5%) since it could only have been as large as I_3. Thus the fluorescence at $\omega_0 + \delta$ was due primarily to collisions.

The effect of radiative trapping,[27] and the pressure, frequency, and intensity dependence of the collisional component, as well as its relation to pressure broadening theory, are the subject of continuing studies.

The authors wish to acknowledge the assistance of M. Raymer in various experimental aspects, and fruitful discussions with W. C. Lineberger and J. Cooper.

---

*Work supported by the National Science Foundation through Grant No. GP-39308X.

†Joint Insititute for Laboratory Astrophysics Visiting Fellow, 1975–1976, on leave of absence from Tel Aviv University.

[1]H. A. Kramers and W. Heisenberg, Z. Phys. 31, 681 (1925).

[2]W. Heitler, *The Quantum Theory of Radiation* (Clarendon Press, Oxford, England, 1957), 3rd ed., pp. 196–204.

[3]D. L. Huber, Phys. Rev. 178, 93 (1969).

[4]A. Omont, E. W. Smith, and J. Cooper, Astrophys. J. 175, 185 (1972).

[5]F. Schuda, C. R. Stroud, Jr., and M. Hercher, J. Phys. B 7, L198 (1974); F. Y. Wu, R. E. Grove, and S. Ezekiel, Phys. Rev. Lett. 35, 1426 (1975).

[6]D. Mihalas, *Stellar Atmospheres* (W. H. Freeman, San Francisco, Calif., 1970), Chap. 10.

[7]J. L. Carlsten and P. C. Dunn, Opt. Commun. 14, 8 (1975).

[8]J. J. Wynne and P. P. Sorokin, J. Phys. B 8, L37 (1975).

[9]P. F. Williams, D. L. Rousseau, and S. H. Dworetsky, Phys. Rev. Lett. 32, 196 (1974).

[10]D. L. Rousseau, G. D. Patterson, and P. F. Williams, Phys. Rev. Lett. 34, 1306 (1975).

[11]L. S. Ditman, Jr., R. W. Gammon, and T. D. Wilkerson, Opt. Commun. 13, 154 (1975).

[12]H. M. Gibbs and T. N. C. Venkatesan, IEEE J. Quantum Electron. 11, 91D (1975).

[13]A. Schabert, R. Keil, and P. E. Toschek, Opt. Commun. 13, 265 (1975).

[14]P. F. Liao and J. E. Bjorkholm, Phys. Rev. Lett. 34, 1 (1975).

[15]D. Prosnitz, E. V. George, and D. Wildman, to be published; W. W. Morey and J. L. Hall, private communication.

[16]S. Mukamel, A. Ben-Reuven, and J. Jortner, Phys. Rev. A 12, 947 (1975); they calculate only the frequency-integrated (total) emission.

[17]B. R. Mollow, Phys. Rev. A 188, 1969 (1969).

[18]A. P. Kazantsev, Zh. Eksp. Teor. Fiz. 66, 1229 (1974) [Sov. Phys. JETP 39, 601 (1974)].

[19]S. S. Hassan and R. K. Bullough, J. Phys. B 8, L147 (1975).

[20]E. V. Baklanov, Zh. Eksp. Teor. Fiz. 65, 2203 (1973) [Sov. Phys. JETP 38, 1100 (1974)]; H. J. Carmichael and D. F. Walls, J. Phys. B 8, L77 (1975).

[21]A. Szöke and E. Courtens, Phys. Rev. Lett. 34, 1053 (1975); B. R. Mollow, Phys. Rev. A 2, 76 (1970).

[22]B. W. Woodard, V. J. Ehlers, and W. C. Lineberger, Rev. Sci. Instrum. 44, 882 (1973).

[23]J. L. Carlsten, J. Phys. B 7, 1620 (1974).

[24]For this calculation, the oscillator strength of the ^1S-^1P transition was taken to be 1.92 as determined by A. Lurio, R. DeZafra, and R. J. Goshen, Phys. Rev. A 134, 1198 (1964).

[25]In a noninverted two-level system the third component has gain. In fact, stimulated emission of the component has been studied by P. P. Sorokiu *et al.*, Appl. Phys. Lett. 10, 44 (1967); N. N. Badalyan, V. A. Iradyan, and M. E. Movsesyan, Zh. Eksp. Teor. Fiz., Pis'ma Red. 8, 518 (1968) [JETP Lett. 8, 316 (1968)]; V. M. Arutyunian *et al.*, Zh. Eksp. Teor. Fiz. 66, 509 (1974) [Sov. Phys. JETP 39, 243 (1974)].

[26]S. Mukamel and J. Jortner, J. Chem. Phys. 62, 3609 (1975); J. M. Friedman and R. M. Hochstrasser, Chem. Phys. 6, 155 (1974); J. O. Berg. C. A. Langhoff, and A. W. Robinson, Chem. Phys. Lett. 29, 305 (1974);

H. Metiu, J. Ross, and A. Nitzan, J. Chem. Phys. 63, 1289 (1975).

[27]M. G. Payne and J. D. Cook, Phys. Rev. A 2, 1238 (1970).

Identification of Absorption Lines by Modulated Lower-Level Population: Spectrum of Na_2 †

M. E. Kaminsky, R. T. Hawkins, F. V. Kowalski, and A. L. Schawlow
Department of Physics, Stanford University, Stanford, California 94305
(Received 2 February 1976)

Molecular absorption lines from a common lower level are intensity modulated by chopped-laser saturation of another line from that level. Populations of some other levels are also modulated by subsequent fluorescence. Both types of modulated lines are free of Doppler broadening. Also, collisional depopulation modulates absorption from rotational levels near the laser-depleted level. In Na_2, we have identified 113 lines. Analysis of the A state by Kusch and Hessel is confirmed and extended.

We present here a new technique for Doppler-free analysis of complicated molecular spectra, which identifies all absorption lines originating in a chosen level. We demonstrate its advantages in studying the $A^1\Sigma_u^+$ state of Na_2. A laser is used to deplete the population of the chosen ground-state level, by exciting a substantial number of the molecules out of that state.[1] The absorption of all lines originating in this same lower level is then decreased. Consequently, if the saturating laser beam is chopped, just these lines are intensity modulated and so distinguished from the many others in the same wavelength region. If the laser is monochromatic and tuned to the center of an absorption line's Doppler profile, the only molecules affected are those with zero component of velocity along the beam direction. Then all the modulated-population spectroscopy (MPS) absorption lines should also be very narrow and essentially without either Doppler broadening or Doppler shift.

In addition to this modulation by lower-level depopulation, which we will call type-1 MPS, there are several secondary ways in which other lines can be modulated (see Fig. 1). The saturating laser excites some molecules to the upper level of the transition which absorbs it. Absorption lines from this level to still higher levels could then be observed. This effect, which we shall call type-2 MPS, is simply stepwise excitation.[2] After the excitation, the molecules fluoresce in some nanoseconds to other vibrational levels of the ground electronic state, and absorption lines from these levels are strengthened when the laser is on. This kind, which we call type-3 MPS, is the probing of the effects of optical pumping. Finally, at higher pressures, collisions transfer molecules from nearby rotational levels to the depopulated one and thereby decrease the population of these neighboring rotational levels when the saturating laser is on. This effect we call type-4 MPS. Modulated-population spectra of types 1, 2, and 3 are Doppler free, while those of type 4 are not. The transmitted probe intensity in types-1 and -4 MPS will be in phase with the chopped saturating laser, while the transmitted intensity in types-2 and -3 MPS will be 180° out of phase. In these experiments, we have observed clear examples of types-1, -3, and -4, and perhaps type-2 MPS.

Sodium vapor was contained in a stainless steel oven with an active region up to 43 cm long, typically operated near 345°C, corresponding to

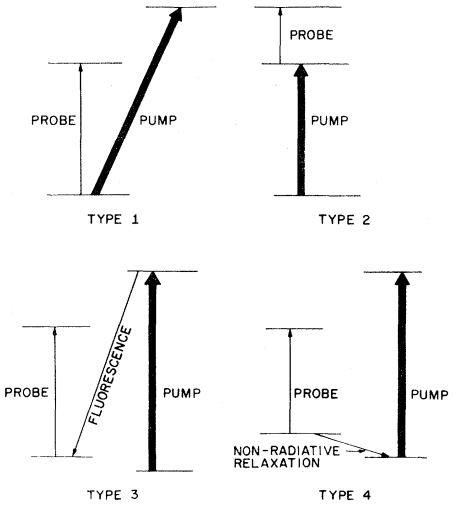

FIG. 1. The four types of modulated-population signals, produced by laser saturation of an absorption line.